Proceedings of 28th International Scientific Conference. Transport Means 2024.

Analysis of Air Dust Pollution in the Transport Compartment of the Launch Vehicle at the Stage of the Pre-launch Preparation

M. Biliaiev[1], V. Biliaieva[2], V. A. Kozachyna[3], V. V. Kozachyna[4], P. Mashykhina[5], P. Semenenko[6]

[1]*Ukrainian State University of Science and Technologies, Lazaryan Str. 2, 49010, Dnipro, Ukraine, E-mail: biliaiev.m@gmail.com*
[2]*Ukrainian State University of Science and Technologies, Lazaryan Str. 2, 49010, Dnipro, Ukraine, E-mail: vikabelyaeva604@gmail.com*
[3]*Ukrainian State University of Science and Technologies, Lazaryan Str. 2, 49010, Dnipro, Ukraine, E-mail: v.kozachyna@gmail.com*
[4]*Ukrainian State University of Science and Technologies, Lazaryan Str. 2, 49010, Dnipro, Ukraine, E-mail: tsurkanvaleri1997@gmail.com*
[5]*Ukrainian State University of Science and Technologies, Lazaryan Str. 2, 49010, Dnipro, Ukraine, E-mail: gidro_eko@ukr.net*
[6]*State Design Office Pivdenne, Kryvorizka Str., 3, 49000, Dnipro, Ukraine, E-mail: semenenkopv1981@gmail.com*
https://doi.org/10.5755/e01.2351-7034.2024.P299-304

Abstract

At the stage of the pre-launch preparation, it is necessary to fulfill very strict environment conditions inside the main fairing where the satellite is located. Namely, it is very important to predict dust concentration inside the main fairing and especially near satellite surface during forced ventilation. To predict air dust pollution inside of main fairing 2D fluid dynamics numerical model has been developed. The governing equations include equation of potential flow to simulate air flow inside the main fairing and equation of pollutant dispersion. Also, empirical model has been used to calculate the number of dust particles fall to the satellite surface. Implicit finite difference schemes of splitting have been used for numerical integration of governing equations. The computer code has been developed on the basis of proposed numerical model. The results of computational experiments to estimate dust concentration field inside the main fairing of the launch vehicle are presented.
KEY WORDS: *satellite, transport compartment, main fairing, air pollution, dust concentration*

1. Introduction

Thermostating of the main fairing volume is a very important procedure at the pre-launch preparatory stage of a launch vehicle (Fig. 1) [1-11]. Long-term air thermostating requires very "strict" conditions for air purity inside the main fairing [5]. Long-term ventilation can lead to dust contamination of the satellite's sensitive surfaces. Particularly sensitive surfaces of the satellite are:

- solar panels;
- optical instruments;
- reflectors of signal transmitters;
- sensitive sensor elements.

Therefore, there is an important task of predicting dust contamination of the satellite inside the main fairing during its forced ventilation.

Fig. 1 Main fairing [12]

2. Mathematical Model

To determine the dust concentration in the main fairing during the forced ventilation, the following problems need to be solved sequentially:

1. Calculate the airflow velocity field in the main fairing.
2. Calculate the dust concentration field in the main fairing.
3. Calculate the number of dust particles that will settle on a "sensitive" surface.

The difficulty of solving these problems lies in the fact that it is necessary to make calculations in a region with complex geometry.

A potential motion model was used to estimate the velocity field in the main fairing during its forced ventilation at the pre-launch stage [1, 13]:

$$\frac{\partial^2 P}{\partial x^2}+\frac{\partial^2 P}{\partial y^2}=0\,, \qquad (1)$$

where P – air flow velocity potential.

The components of the airflow velocity vector are determined on the basis of dependencies (2):

$$u=\frac{\partial P}{\partial x}, v=\frac{\partial P}{\partial y}\,. \qquad (2)$$

Boundary conditions for Eq. (1) are as follows:

1. $\frac{\partial P}{\partial x}=V_{in}$ – at the inlet boundary (V_{in} is air flow speed at this boundary).
2. P = Const – at the outlet boundary.
3. $\frac{\partial P}{\partial n}=0$ – is outward normal to the solid surface.

To predict the level of dust contamination of the launch vehicle's main fairing during the forced venting procedure, the dust particle transfer equation was used [1,13]:

$$\frac{\partial C}{\partial t}+\frac{\partial uC}{\partial x}+\frac{\partial vC}{\partial y}=\frac{\partial}{\partial x}\left(\mu_x\frac{\partial C}{\partial x}\right)+\frac{\partial}{\partial y}\left(\mu_y\frac{\partial C}{\partial y}\right), \qquad (3)$$

where C – dust concentration, mg/m^3; u, v – components of the air velocity vector in the main fairing, m/s; t – time, s; μ_x, μ_y – diffusion coefficients, m^2/s.

The boundary conditions for Eq. (3) are as follows:

1. At the entrance to the main fairing: $C=C_{in}$, where C_{in} – known dust concentration.
2. At the air outlet from the main fairing: $C_{ij}=C_{out}$, where C_{out} – dust concentration in the last computing cell; C_{ij} – dust concentration in the next to last computing cell.
3. On hard surfaces of the main fairing and the satellite floor:

$$\frac{\partial C}{\partial n}=0\,,$$

where n – unit normal to the surface.

The initial conditions for t=0 are as follows: $C=C_0$, where C_0 – known dust concentration in the main fairing. The diffusion coefficients were determined as follows:

$$\mu_x=k_0\cdot u, \mu_y=k_0\cdot v, k_0=0.1.$$

To solve the problem of aerodynamics Eq. (1), the Laplace equation was reduced to the form:

$$\frac{\partial P}{\partial t}=\frac{\partial^2 P}{\partial x^2}+\frac{\partial^2 P}{\partial y^2}\,, \qquad (4)$$

where t – fictitious time.

Before solving Eq. (4), an initial condition needs to be set for fictitious time, for example, P=0 for t=0.

Next, the change-triangle method to solve Eq. (4) was used. This is a two-step method for solving the problem numerically. The first step to solve is the following equation:

$$\frac{P_{i,j}^{n+1/2}-P_{i,j}^{n}}{0.5\Delta t}=\frac{P_{i+1,j}^{n}-P_{i,j}^{n}}{\Delta x^2}+\frac{-P_{i,j}^{n+\frac{1}{2}}+P_{i-1,j}^{n+\frac{1}{2}}}{\Delta x^2}+\frac{P_{i,j+1}^{n}-P_{i,j}^{n}}{\Delta y^2}+\frac{-P_{i,j}^{n+\frac{1}{2}}+P_{i,j-1}^{n+\frac{1}{2}}}{\Delta y^2}.$$

The second step to solve is the following equation:

$$\frac{P_{i,j}^{n+1}-P_{i,j}^{n+1/2}}{0.5\Delta t}=\frac{P_{i+1,j}^{n+1}-P_{i,j}^{n+1}}{\Delta x^2}+\frac{-P_{i,j}^{n+\frac{1}{2}}+P_{i-1,j}^{n+\frac{1}{2}}}{\Delta x^2}+\frac{P_{i,j+1}^{n+1}-P_{i,j}^{n+1}}{\Delta y^2}+\frac{-P_{i,j}^{n+\frac{1}{2}}+P_{i,j-1}^{n+\frac{1}{2}}}{\Delta y^2}.$$

The value of the velocity potential at each step was determined by an explicit formula at each step. The calculation ends when the following condition is fulfilled:

$$\left|P_{i,j}^{n+1}-P_{i,j}^{n}\right|\le\varepsilon,$$

where ε – a small number. In calculations ε =0.01 was assumed; n – iteration number.

Next, the air flow velocity components were calculated using the following formulas:

$$u_{ij}=\frac{P_{i,j}-P_{i-1,j}}{\Delta x},\ v_{ij}=\frac{P_{i,j}-P_{i,j-1}}{\Delta y}.$$

For numerical integration of Eq. (3), the derivatives were approximated as follows:

$$\frac{\partial uC}{\partial x}=\frac{\partial u^+C}{\partial x}+\frac{\partial u^-C}{\partial x},$$

$$\frac{\partial vC}{\partial y}=\frac{\partial v^+C}{\partial y}+\frac{\partial v^-C}{\partial y},$$

$$u^+=\frac{u+|u|}{2},\ u^-=\frac{u-|u|}{2},\ v^+=\frac{v+|v|}{2},\ v^-=\frac{v-|v|}{2}.$$

$$\frac{\partial u^+C}{\partial x}\approx\frac{u_{i+1,j}^{+}C_{ij}^{n+1}-u_{ij}^{+}C_{i-1,j}^{n+1}}{\Delta x}=L_x^+C^{n+1},$$

$$\frac{\partial u^-C}{\partial x}\approx\frac{u_{i+1,j}^{-}C_{i+1,j}^{n+1}-u_{ij}^{-}C_{ij}^{n+1}}{\Delta x}=L_x^-C^{n+1},$$

$$\frac{\partial \text{v}^+C}{\partial y}\approx\frac{\text{v}_{i,j+1}^{+}C_{ij}^{n+1}-\text{v}_{ij}^{+}C_{i,j-1}}{\Delta y}=L_y^+C^{n+1}$$

$$\frac{\partial \text{v}^-C}{\partial y}\approx\frac{\text{v}_{i,j+1}^{-}C_{i,j+1}^{n+1}-\text{v}_{ij}^{-}C_{ij}^{n+1}}{\Delta y}=L_y^-C^{n+1}$$

$$\frac{\partial C}{\partial t}\approx\frac{C_{ij}^{n+1}-C_{ij}^{n}}{\Delta t},$$

$$\frac{\partial}{\partial x}(\mu_x\frac{\partial C}{\partial x})\approx\tilde{\mu}_x\frac{C_{i+1,j}^{n+1}-C_{ij}^{n+1}}{\Delta x^2}-\tilde{\mu}_x\frac{C_{ij}^{n+1}-C_{i-1,j}^{n+1}}{\Delta x^2}=M_{xx}^-C^{n+1}+M_{xx}^+C^{n+1},$$

$$\frac{\partial}{\partial y}(\mu_y\frac{\partial C}{\partial y})\approx\tilde{\mu}_y\frac{C_{i,j+1}^{n+1}-C_{ij}^{n+1}}{\Delta y^2}-\tilde{\mu}_y\frac{C_{ij}^{n+1}-C_{i,j-1}^{n+1}}{\Delta y^2}=M_{yy}^-C^{n+1}+M_{yy}^+C^{n+1}.$$

Then the analog of the mass transfer Eq. (3) can be written as follows:

$$\frac{C_{ij}^{n+1}-C_{ij}^{n}}{\Delta t}+L_x^{+}C^{n+1}+L_x^{-}C^{n+1}+L_y^{+}C^{n+1}+L_y^{-}C^{n+1}= \\ =M_{xx}^{+}C^{n+1}+M_{xx}^{-}C^{n+1}+M_{yy}^{+}C^{n+1}+M_{yy}^{-}C^{n+1}. \quad (5)$$

To solve the problem of determining the dust concentration, Eq (5) was split as follows:

1. step 1 (k=1/4):

$$\frac{C_{ij}^{n+k}-C_{ij}^{n}}{\Delta t}+\frac{1}{2}(L_x^{+}C^{k}+L_y^{+}C^{k})= \\ =\frac{1}{4}(M_{xx}^{+}C^{k}+M_{xx}^{-}C^{k}+M_{yy}^{+}C^{n}+M_{yy}^{-}C^{n}); \quad (6)$$

2. step 2 (k=n+1/2; c=n+1/4):

$$\frac{C_{ij}^{k}-C_{ij}^{c}}{\Delta t}+\frac{1}{2}(L_x^{-}C^{k}+L_y^{-}C^{k})= \\ =\frac{1}{4}(M_{xx}^{-}C^{k}+M_{xx}^{+}C^{c}+M_{yy}^{-}C^{k}+M_{yy}^{+}C^{c}); \quad (7)$$

3. step 3 (k=n+3/4; c=n+1/2):

$$\frac{C_{ij}^{k}-C_{ij}^{c}}{\Delta t}+\frac{1}{2}(L_x^{+}C^{k}+L_y^{-}C^{k})= \\ =\frac{1}{4}(M_{xx}^{-}C^{c}+M_{xx}^{+}C^{k}+M_{yy}^{-}C^{k}+M_{yy}^{+}C^{c}); \quad (8)$$

4. step 4 (k=n+1; c=n+3/4):

$$\frac{C_{ij}^{k}-C_{ij}^{c}}{\Delta t}+\frac{1}{2}(L_x^{-}C^{k}+L_y^{+}C^{k})= \\ =\frac{1}{4}(M_{xx}^{-}C^{k}+M_{xx}^{+}C^{c}+M_{yy}^{-}C^{c}+M_{yy}^{+}C^{k}). \quad (9)$$

The dust concentration in Eq. (6) – Eq. (9) was determined by the explicit formula.

To calculate the number of dust particles that have a size of more than 5 μm and fall on the horizontal surface, an empirical model was used [9]:

$$C_s = c\cdot p\cdot C_n^{0.773}t,$$

where c = 1.076 – empirical coefficient, t – time, p = 2.851 – empirical coefficient [9]; C_n – concentration of dust in the air near the sensitive surface.

The code was created on the basis of the developed numerical model, the programming language is FORTRAN.

3. Results

This section presents the results of numerical experiments which were carried out using developed numerical models. Computational experiments were carried out for satellites inside CYCLONE-IV launch vehicle main fairing. Two cases were considered in which the satellite had complex geometrical shape (Fig. 2 and Fig. 4). The main fairing dimensions of this launch vehicle were 4.99m×4m (two-dimensional model). A uniform air flow was set at the upper boundary of the computational region, with a velocity of 3 m/s. Diameter of dust particles which enter the main fairing was 7 μm. Dust concentration in the air flow which was used for forced ventilation was 10^4 particles/m^3. Results of numerical experiment are shown in Fig. 3 and Fig. 5. These Figures show concentration in dimensionless form: each number in these Figures show the concentration as the percentage of the maximum concentration in the computational region.

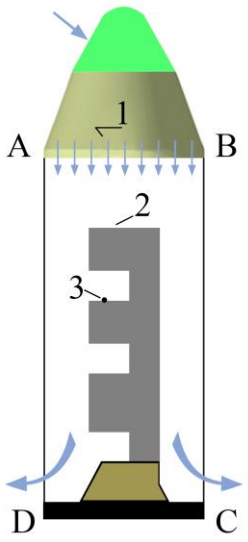

Fig. 2 Computational region sketch (Case #1): 1 – inlet boundary; 2 – satellite; 3 – sensitive surface

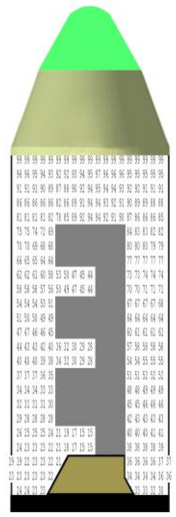

Fig. 3 Dust concentration (dimensionless) in main fairing (Case #1)

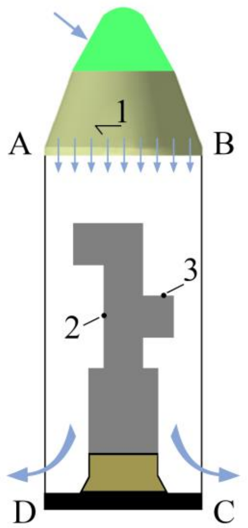

Fig. 4 Computational region sketch (Case #2): 1 – inlet boundary; 2 – satellite; 3 – sensitive surface

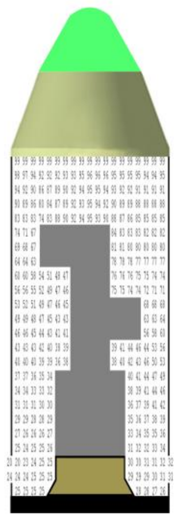

Fig. 5 Dust concentration (dimensionless) in main fairing (Case #2)

Results of numerical experiment show that satellite geometrical form influences strictly on the dust distribution inside the main fairing. For Case #1 dust concentration at the left opening is about 19%–23% of the maximum dust concentration inside the main fairing and for the right opening it is about 36%–37%. For Case #2 dust concentration at the left opening is about 20%–24% of the maximum dust concentration inside the main fairing and for the right opening it is about 31%–32%. Amount of dust particles which fall on the sensitive surfaces after 1 day forced ventilation is shown in Table 1.

Table 1

Number of particles which set on the sensitive surface

Case #1	Case #2
46 particles	630 particles

Results from Table 1 show that for Case #2 it will be intensive dust pollution of the sensitive surface. It is connected with the location of this surface: it is situated on the "windward" side of the satellite element. Air flow "collides" this surface and this causes dust particles fall on it. In Case #1 the sensitive surface is situated behind the satellite element which "works" as an obstacle and protects sensitive surface from pollution.

Worthy of note that computational time was 8s.

4. Conclusions

A quick-computing numerical model was developed to predict dust pollution inside the main fairing of the launch vehicle during its forced ventilation. Proposed numerical model allows to take into account the main physical factors which influence dust distribution inside main fairing during forced ventilation. The developed computer program makes it possible to carry out computational calculations in a short time. This computer program can be used for the initial assessment of the dust regime in the main fairing at the stage of its forced ventilation.

References

1. **Biliaiev, M.; Biliaieva, V.; Rusakova, T.; Kozachyna, V.A.; Berlov, O.; Semenenko, P.; Kozachyna, V.V.; Brazaluk, I.; Klym, V.; Tatarko, L.** 2022. Development of a Method for Assessing Air Dustiness in the Main Fairing of the Launch Vehicle, Eastern-European Journal of Enterprise Technologies 5/1(119): 17–25.
2. Compartment venting – Space vehicle design criteria. NASA-SP-8060 [online cit.: 2024-05-12]. Available from: https://ntrs.nasa.gov/citations/19710018690
3. Falcon User’s Guide. Space Exploration Technologies Corp [online cit.: 2024-05-14]. Available from: https://cutt.ly/WettMMly
4. **Groves, C. E.** 2014. Computational Fluid Dynamics Uncertainty Analysis for Payload Fairing Spacecraft Environmental Control Systems. Doctoral dissertation, University of Central Florida, 185 p.
5. **Кашанов, А.Э.; Дегтярев, А.В.; Гладкий, Э.Г.; Баранов, Е.Ю.** 2012. Оценка технических рисков при пуске ракеты-носителя «Днепр», Авиационно-космическая техника и технология 5 (92): 113–117. (in Russian).
6. LM-3A Series Launch Vehicle User’s Manual (2011) [online cit.: 2024-05-20]. Available from: https://www.cgwic.com/LaunchServices/Download/manual/
7. **Mehta, R.C.** 2017. Analysis of payload compartment venting of satellite launch vehicle, Advances in Aircraft and Spacecraft Science 4(4): 437-448.
8. **Nallasamy, R.; Kandula, M.; Duncil, L.; Schallhorn, P.** 2008. Three-Dimensional Flowfield in the Scaled Payload/Fairing Model of an Expendable Launch Vehicle, 38th Fluid Dynamics Conference and Exhibit, Washington: 1–21.
9. **Tribble, A. C.; Boyadjan, B.; Davis, J. et al.** 1996. Contamination Control Engineering Design Guidelines the Aerospace Community. NASA.
10. **Bulavka, S. S.** 2021. Experimental results of an advanced thermostat system the air of launch vehicles, Naukovi notatki, 71: 9–15.
11. **Zgurovsky, M.Z.; Skopetsky, V.V.; Khrutch, V.K.; Biliaiev, M.M.** 1997. Numerical modeling of pollution dispersion in environment. Kyiv: Naukova dumka, 368 p.
12. Fairing Installation and Transfer of PRISMA Satellite, the 14th Vega Launch [online cit.: 2024-05-08]. Available from: https://cutt.ly/uetrDluX
13. **Vanhove, E.; Tondu, T.; Roussel, J. F.; Faye, D.; Guigue, P.** 2016. In Situ Real-Time Quantitative and Qualitative Monitoring of Molecular Contamination.,Journal of Spacecraft and Rockets 53(6): 1166–1171.